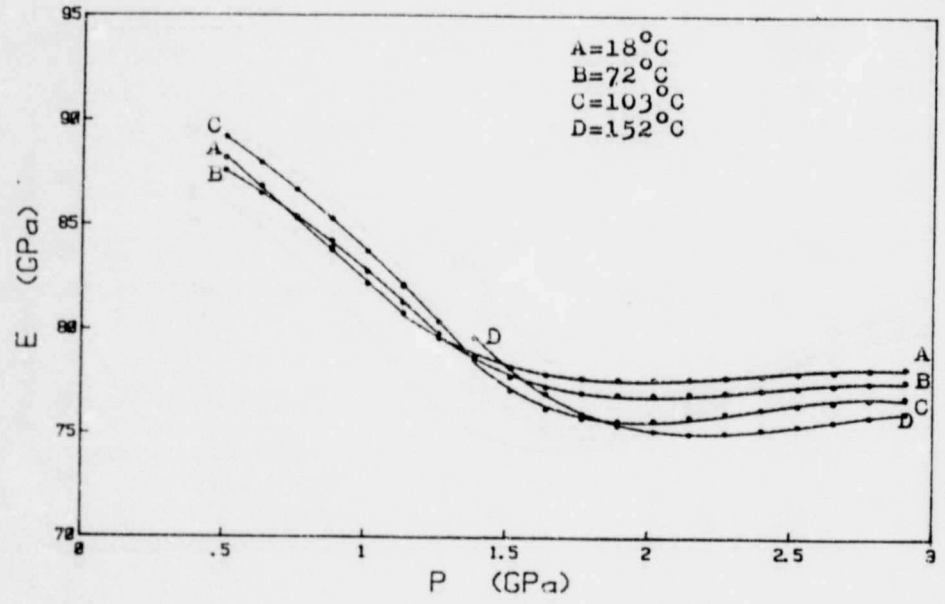

Fig. 5.1.8 Zerodur: Young's modulus (E) vs pressure

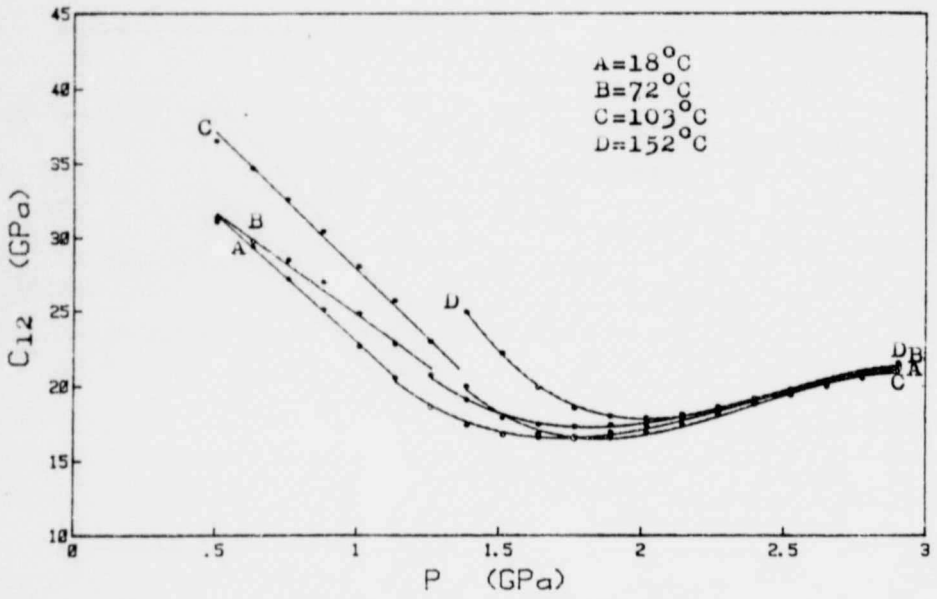

Fig. 5.1.9 Zerodur: Lamé constant (C_{12}) vs pressure

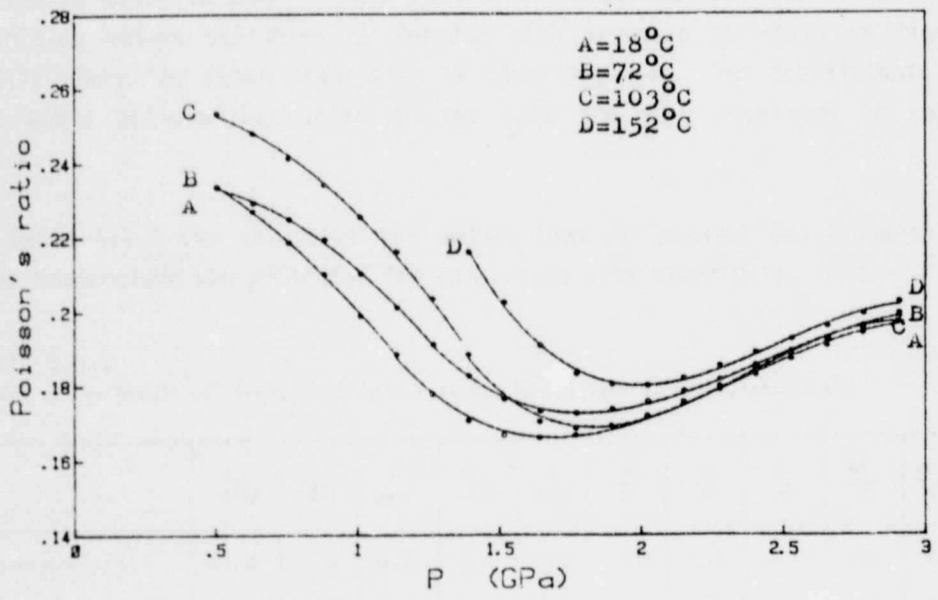

Fig. 5.1.10 Zerodur: Poisson's ratio (σ) vs pressure

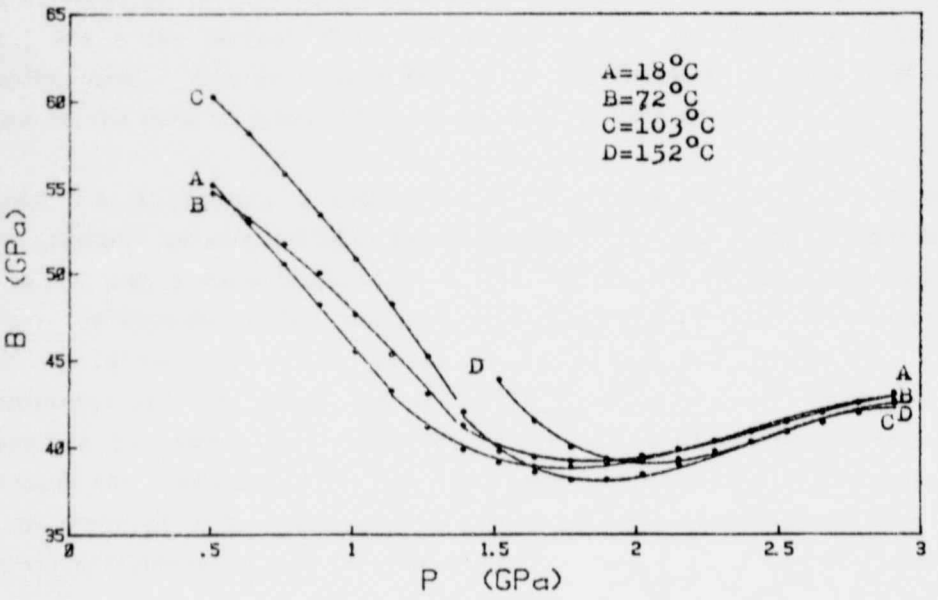

Fig. 5.1.11 Zerodur: Bulk modulus (B) vs pressure

quasi-linear section and a curved section and appropriate polynomials were fitted to describe them. These results are compiled in table 5.1.2. The resulting volume variation of Zerodur with pressure is shown in figure 5.1.12 where the phase transition is clearly shown. The coefficients of the cubic polynomials fitted to the data are also displayed in table 5.1.2.

In table 5.1.3 the values of the moduli from the present measurements at room temperature are presented for comparison with other data.

Table 5.1.3
Values of the Moduli of Zerodur and their Pressure Derivatives at Room Conditions

	C_{11} (GPa)	C_{44} (GPa)	E (GPa)	C_{12} (GPa)	B (GPa)	$\frac{dL}{dP}$	$\frac{dG}{dP}$	$\frac{dC_{11}}{dP}$	$\frac{dC_{44}}{dP}$	$\frac{dC_{12}}{dP}$	$\frac{dB}{dP}$
Present Work (18°C)	113,30	37,21	94,20	40,27	65,04	-21,79	-3,15	-21,28	-2,91	-17,32	-19,19
Gerlich & Wolf (op cit)	104,9	36,20	89,53	32,50	56,63	-16,33	-2,96	-15,71	-2,75	-10,22	-12,05
Schott data		37	92								

The differences in this work compared to the work of Gerlich and Wolf (op. cit.) are a few percent which are mainly due to the different batch of samples used. However, the values of G and E for this study are more close to the data of Schott than in the case of Gerlich and Wolf.

Figure 5.1.13 presents a comparison of the volume variation of Zerodur with pressure as measured with two different techniques. The present work at 18 °C and a room temperature static-compression method developed by Vaidya and Kennedy (1970), and used by Sigalas et al. (1985) to determine the variation for this material (Sigalas and Auret, private communication). It shows the reliability of the present measurements; where the two curves agree at 3 GPa to within 1 % of volume compression, although the compressibility technique used in this laboratory is subject to an error of 7 %. However, this does not completely account for the overall difference between the two curves.

Table 5.1.2

Zerodur glass ceramic: Elastic Properties and their Polynomial Coefficients
Density = 2,537 g/cc v_ℓ = 6,532 km/s v_t = 3,792 km/s

ELASTIC CONSTANT	TEMPERATURE (°C)	COEFFICIENTS OF EQUATION $M = a_0 + a_1P + a_2P^2 + a_3P^3$				$X \leq P \leq Y$(GPa)	
		a_0	$a_1(GPa^{-1})$	$a_2(GPa^{-2})$	$a_3(GPa^{-3})$	X	Y
C_{11}(GPa)	18	113,30	-21,28			0,5	1,4
		122,20	-53,44	23,29	-3,17	1,4	3
	72	108,96	-11,35	-4,14		0,5	1,4
		139,97	-76,06	32,60	-4,41	1,4	3
	103	115,99	-13,64	-5,66		0,5	1,4
		188,05	-143,9	62,80	-8,77	1,4	3
	152	112,04	-7,79	-5,51		0,5	1,4
		217,53	-170,42	69,56	-9,17	1,4	3
C_{44}(Gpa)	18	37,21	-2,91			0,5	1
		37,44	-4,68	1,75	-0,24	1	3
	72	36,83	-2,62			0,5	1,26
		38,89	-7,40	3,00	-0,42	1,26	3
	103	37,07	-2,89			0,5	1,39
		42,23	-12,31	5,08	-0,71	1,39	3
	152	40,10	-8,63	2,89	-0,32	1,5	3
E (GPa)	18	94,20	-11,81			0,5	1,14
		105,14	-36,81	16,02	-2,25	1,14	3
	72	90,62	-4,44	-3,27		0,5	1,26
		112,16	-46,44	19,91	-2,77	1,26	3
	103	92,90	-5,71	-3,31		0,5	1,39
		133,26	-76,51	33,12	-4,64	1,39	3
	152	134,33	-71,46	28,14	-3,59	1,39	3

(Continue)

ELASTIC CONSTANT	TEMPERATURE (°C)	COEFFICIENTS OF EQUATION $M = a_0 + a_1P + a_2P^2 + a_3P^3$				$X \leq P \leq Y$(GPa)	
		a_0	$a_1(GPa^{-1})$	$a_2(GPa^{-2})$	$a_3(GPa^{-3})$	X	Y
C_{12}(GPa)	18	40,27	-17,32			0,5	1,4
		63,70	-67,68	30,90	-4,35	1,14	3
	72	38,55	-13,79			0,5	1,26
		71,07	-73,78	32,34	-4,42	1,26	3
	103	46,46	-18,59			0,5	1,39
		103,59	-119,28	52,63	-7,36	1,39	3
	152	140,67	-157,70	65,80	-8,83	1,39	3
	18	$2,50 \times 10^{-1}$	$-1,45 \times 10^{-2}$	$-3,53 \times 10^{-2}$		0,5	1,14
		$4,52 \times 10^{-1}$	$-4,17 \times 10^{-1}$	$1,93 \times 10^{-1}$	$-2,74 \times 10^{-2}$	1,14	3
	72	$2,32 \times 10^{-1}$	$2,54 \times 10^{-2}$	$-4,61 \times 10^{-2}$		0,5	1,26
		$4,87 \times 10^{-1}$	$-4,36 \times 10^{-1}$	$1,93 \times 10^{-1}$	$-2,65 \times 10^{-2}$	1,26	3
	103	$2,55 \times 10^{-1}$	$1,85 \times 10^{-2}$	$-4,76 \times 10^{-2}$		0,5	1,39
		$6,95 \times 10^{-1}$	$-7,27 \times 10^{-1}$	$3,23 \times 10^{-1}$	$-4,55 \times 10^{-1}$	1,39	3
	152	$8,48 \times 10^{-1}$	$-8,64 \times 10^{-1}$	$3,62 \times 10^{-1}$	$-4,87 \times 10^{-2}$	1,39	3
B (GPa)	18	65,01	-19,19			0,5	1,14
		88,22	-70,14	31,74	-4,47	1,14	3
	72	59,85	-7,82	-4,17		0,5	1,39
		90,43	-69,46	30,11	-4,07	1,39	3
	103	66,77	-10,27	-5,41		0,5	1,39
		131,75	-127,49	56,02	-7,83	1,39	3
	152	64,85	-4,40	-6,18		0,5	1,52
		165,47	-160,82	66,56	-8,87	1,52	3
V/V_o	18	$9,987 \times 10^{-1}$	$-1,07 \times 10^{-2}$	$-7,61 \times 10^{-3}$	$1,38 \times 10^{-3}$	0,5	3
	72	$9,979 \times 10^{-1}$	$-0,99 \times 10^{-2}$	$-7,57 \times 10^{-3}$	$1,31 \times 10^{-3}$	0,5	3
	103	$9,969 \times 10^{-1}$	$-0,50 \times 10^{-2}$	$-10,03 \times 10^{-3}$	$1,68 \times 10^{-3}$	0,5	3
	152	$9,969 \times 10^{-1}$	$-0,59 \times 10^{-2}$	$-8,28 \times 10^{-2}$	$1,26 \times 10^{-3}$	0,5	3

ELASTIC CONSTANT	TEMPERATURE (°C)	COEFFICIENTS OF EQUATION $M = a_0 + a_1P + a_2P^2 + a_3P^3$				$X \leq P \leq Y$(GPa)	
		a_0	a_1(GPa^{-1})	a_2(GPa^{-2})	a_3(GPa^{-3})	X	Y
C_{12}(GPa)	18	40,27	-17,32			0,5	1,4
		63,70	-67,68	30,90	-4,35	1,14	3
	72	38,55	-13,79			0,5	1,26
		71,07	-73,78	32,34	-4,42	1,26	3
	103	46,46	-18,59			0,5	1,39
		103,59	-119,28	52,63	-7,36	1,39	3
	152	140,67	-157,70	65,80	-8,83	1,39	3
	18	$2,50 \times 10^{-1}$	$-1,45 \times 10^{-2}$	$-3,53 \times 10^{-2}$		0,5	1,14
		$4,52 \times 10^{-1}$	$-4,17 \times 10^{-1}$	$1,93 \times 10^{-1}$	$-2,74 \times 10^{-2}$	1,14	3
	72	$2,32 \times 10^{-1}$	$2,54 \times 10^{-2}$	$-4,61 \times 10^{-2}$		0,5	1,26
		$4,87 \times 10^{-1}$	$-4,36 \times 10^{-1}$	$1,93 \times 10^{-1}$	$-2,65 \times 10^{-2}$	1,26	3
	103	$2,55 \times 10^{-1}$	$1,85 \times 10^{-2}$	$-4,76 \times 10^{-2}$		0,5	1,39
		$6,95 \times 10^{-1}$	$-7,27 \times 10^{-1}$	$3,23 \times 10^{-1}$	$-4,55 \times 10^{-1}$	1,39	3
	152	$8,48 \times 10^{-1}$	$-8,64 \times 10^{-1}$	$3,62 \times 10^{-1}$	$-4,87 \times 10^{-2}$	1,39	3
B (GPa)	18	65,01	-19,19			0,5	1,14
		88,22	-70,14	31,74	-4,47	1,14	3
	72	59,85	-7,82	-4,17		0,5	1,39
		90,43	-69,48	30,11	-4,07	1,39	3
	103	66,77	-10,27	-5,41		0,5	1,39
		131,75	-127,49	56,02	-7,83	1,39	3
	152	64,85	-4,40	-6,18		0,5	1,52
		165,47	-160,82	66,56	-8,87	1,52	3
V/V_o	18	$9,987 \times 10^{-1}$	$-1,07 \times 10^{-2}$	$-7,61 \times 10^{-3}$	$1,38 \times 10^{-3}$	0,5	3
	72	$9,979 \times 10^{-1}$	$-0,99 \times 10^{-2}$	$-7,57 \times 10^{-3}$	$1,31 \times 10^{-3}$	0,5	3
	103	$9,969 \times 10^{-1}$	$-0,50 \times 10^{-2}$	$-10,03 \times 10^{-3}$	$1,68 \times 10^{-3}$	0,5	3
	152	$9,969 \times 10^{-1}$	$-0,59 \times 10^{-2}$	$-8,28 \times 10^{-2}$	$1,26 \times 10^{-3}$	0,5	3

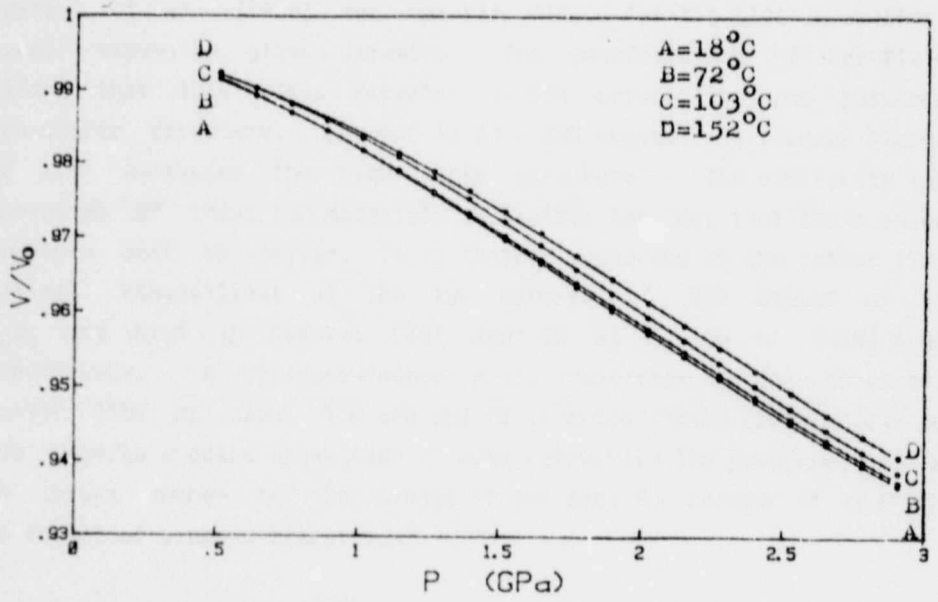

Fig. 5.1.12 Zerodur: Volume variation (V/V_0) vs pressure

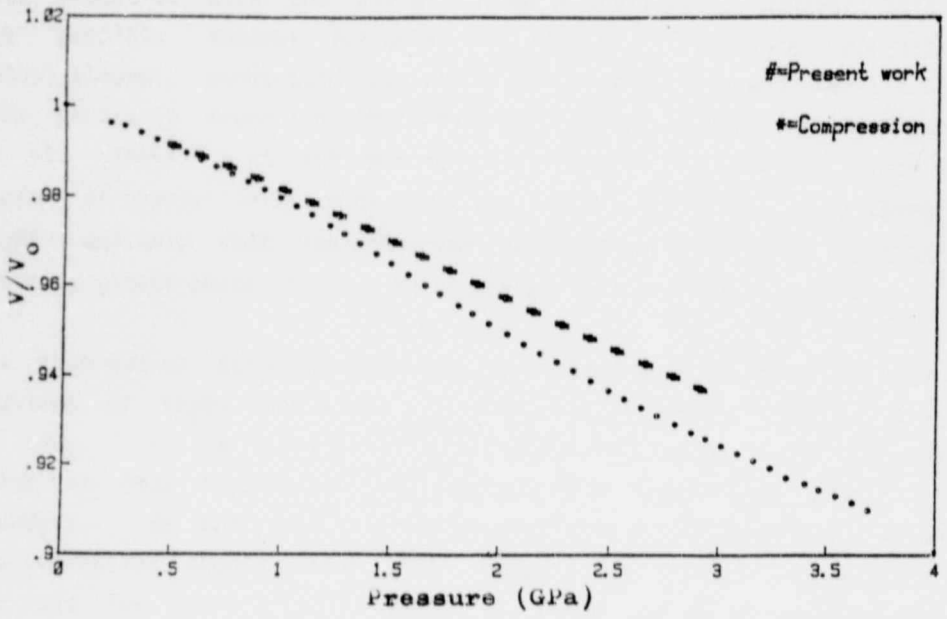

Fig. 5.1.13 Zerodur: Volume variation vs pressure at room temperature as measured with the ultrasonic method and the static-compression method

The values of the elastic constants of Zerodur and their pressure derivatives at zero pressure are very similar to the ones obtained by Sigalas, et al. (1985) for Cer-Vit C101. Cer-Vit C101 is another low thermal expansion glass ceramic. The manufacturers of Cer-Vit C101 claimed that this glass ceramic is 95% crystalline and possesses a high-quartz structure. Zerodur is 70 - 80% crystalline (Jenaer Glaswerk) and also possesses the high-quartz structure. The similarity in the properties of these two materials emphasizes the fact that their internal structure must be similar. It is further supported by the rather similar chemical compositions of the two materials. The amount of SiO_2, Al_2O_3 and Li_2O in Cer-Vit C101 are 68 wt %, 20 wt % and 4 wt %, respectively. A pressure-induced phase transition has been observed for Cer-Vit C101 at about 1.0 GPa and it is quite likely that Zerodur would also undergo a phase transition at some relatively low pressure. In fact, the abrupt change in the slopes of the data for Zerodur at ~1.5 GPa is the result of a phase transition.

An attempt has been made by Sigalas, et al. (private communication) to confirm the phase transition in Cer-Vit C101, using X-ray diffraction at high pressures with the aid of a diamond anvil cell. However, this was not possible because molecules of the fluid pressure transmitter, methyl-alcohol, penetrated into the crystalline structure of Cer-Vit C101, thus partially cancelling the effect of pressure as explained by Mirwald, et al. (1984). An SEM micrograph of Cer-Vit C101 showed a very high degree of crystallinity which would not be less than 95%. It is therefore highly unlikely that the observed phase transition takes place in the minority glassy phase, it must be occurring in the crystalline one.

The high-quartz structure has been stabilized to room temperature by the addition of Al_2O_3 and Li_2O. Figure 5.1.14 shows the phase diagram of SiO_2. It is quite likely that the stabilization of the high-quartz phase at room temperature would lower the low-to-high quartz phase boundary. In that case, at room temperature, a high-to-low quartz phase transformation should occur with increase in pressure, i.e. the one observed for Cer-Vit C101. As all the properties of Zerodur are similar to Cer-Vit C101, Zerodur should undergo a phase transformation similar to

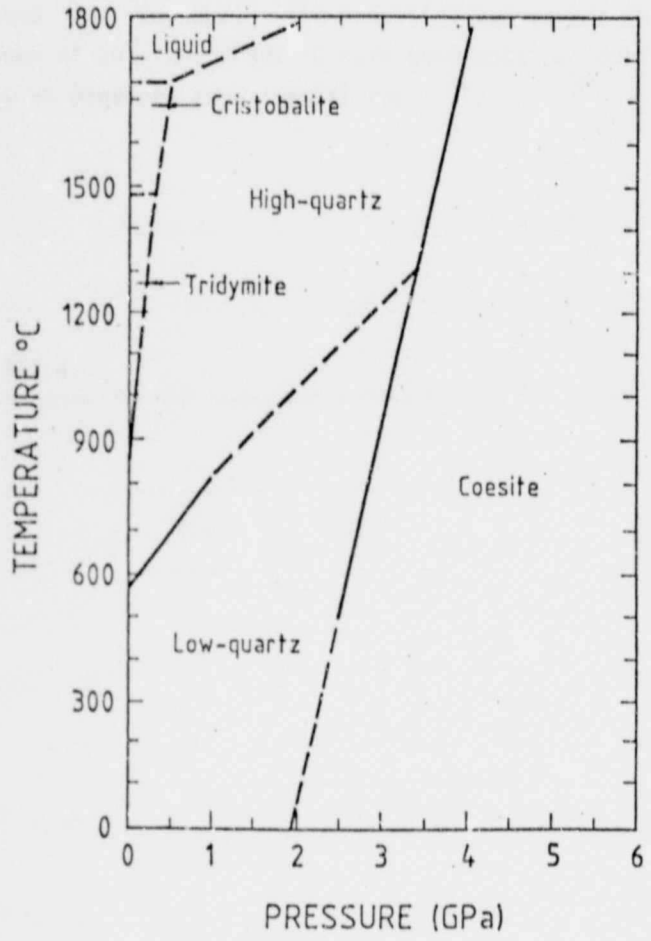

Fig. 5.1.14 Phase diagram of SiO_2 (after Sigalas, et al., 1985)

the one by Cer-Vit C101, i.e. the high-to-low quartz phase transformation at ~1.5 GPa.

Considering now the exact pressure values where the discontinuities start for each of the isotherms, the high-to-low quartz phase boundary can be established for Zerodur. The resulting values are shown in table 5.1.4. The values of 201 °C and 302 °C have been obtained during the longitudinal frequency vs pressure experimental run.

Table 5.1.4
Values Indicating the High-to-Low Quartz Phase Boundary for Zerodur

T(°C)	P(GPa)
18	1,25
72	1,4
103	1,6
152	1,8
201	2,1
302	2,55

Figure 5.1.15 then represents the phase diagram for Zerodur in the 0-300 °C temperature range and 0-3 GPa pressure range. This kind of result stresses the multilateral application of this experimental technique.

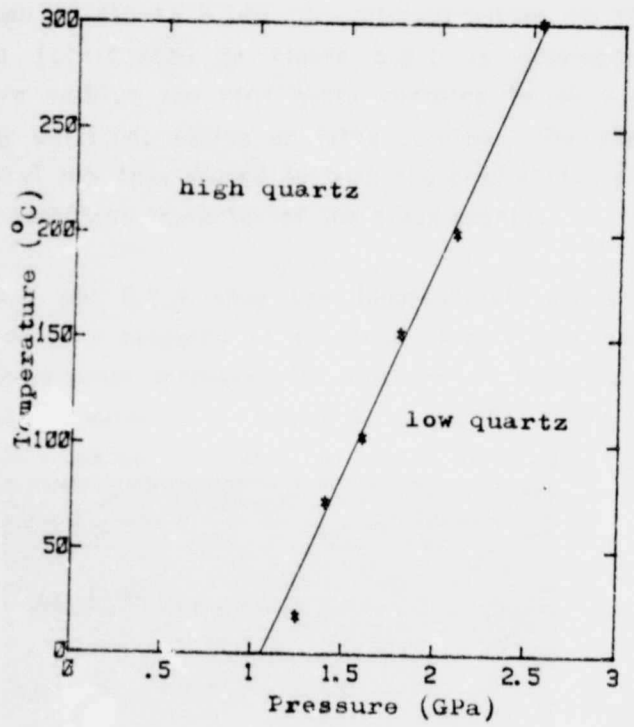

Fig. 5.1.15 Phase diagram of Zerodur

5.2 Corning 9658 glass ceramic

The elastic properties of this glass ceramic were measured and calculated for the following isotherms: 19 °C, 104 °C, 151 °C and 229 °C. This material is a machinable glass ceramic, consisting of a network of fluorophlogopite mica crystallites, $KMg_3AlSi_2O_{10}F_2$, (about 50 % by volume) embedded in a matrix of boro-alumino-silicate glass (Harrington, et al., 1980). The crystallites are approximately 2 μ thick and 5 - 20 μ square and are interlocked and randomly oriented. After a crystallisation heat treatment at 950 to 1 050 °C a microstructure of interlocking mica crystals as illustrated in figure 5.2.1 is developed. The unique microstructure enables the mica glass ceramics to be machined to close tolerances by drilling, sawing or lathe turning. The elastic properties of the material may thus depend on both the crystalline properties of the mica and the amorphous character of the glass matrix.

Figures 5.2.2 and 5.2.3 show the longitudinal and shear frequencies against pressure as measured at the four temperatures and corrected for friction. These modes increase with pressure which is the usual behaviour for a crystalline material. Figures 5.2.4 and 5.2.5 are the longitudinal and shear moduli against pressure, calculated by using the above data.

Fig. 5.2.1 Electron micrograph of a machinable glass ceramic (after McMillan, 1979)

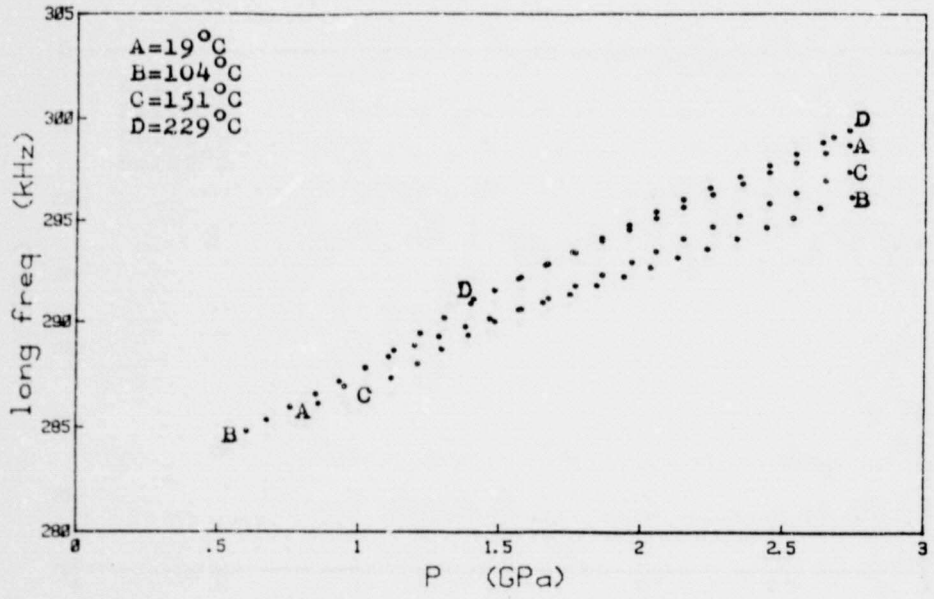

Fig. 5.2.2 9658 glass ceramic (GC): Isotherms for the longitudinal frequency vs pressure

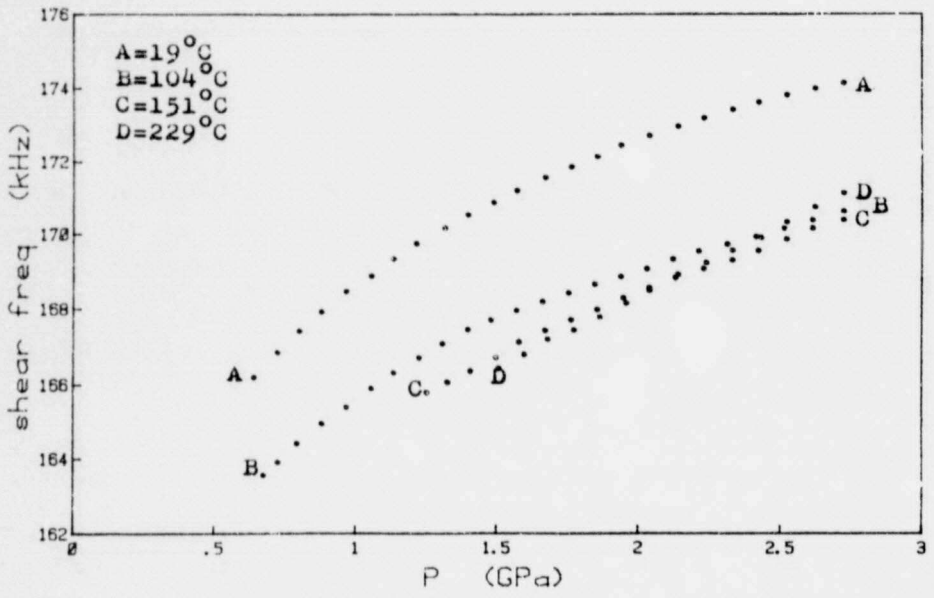

Fig. 5.2.3 9658 GC: Isotherms for the shear frequency vs pressure

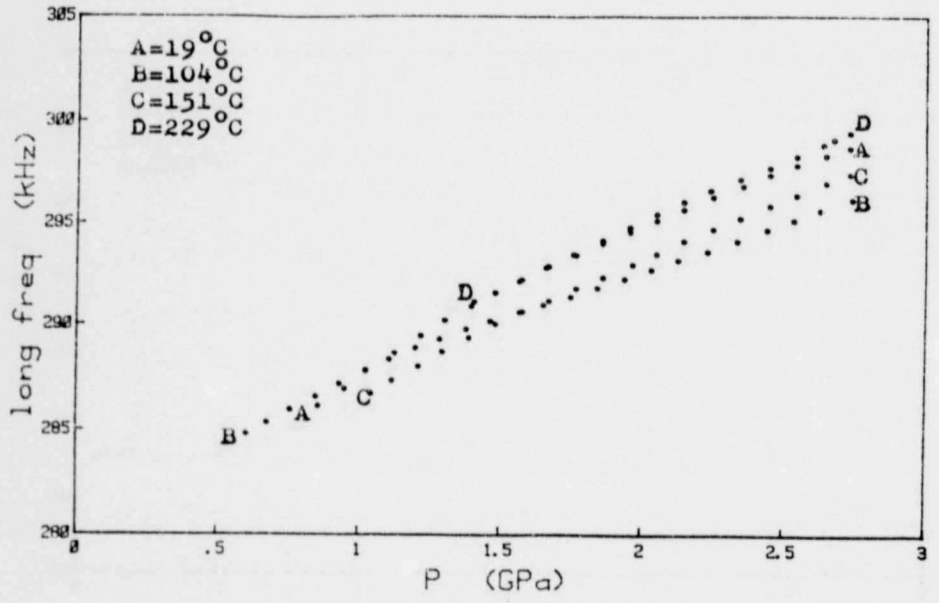

Fig. 5.2.2 9658 glass ceramic (GC): Isotherms for the longitudinal frequency vs pressure

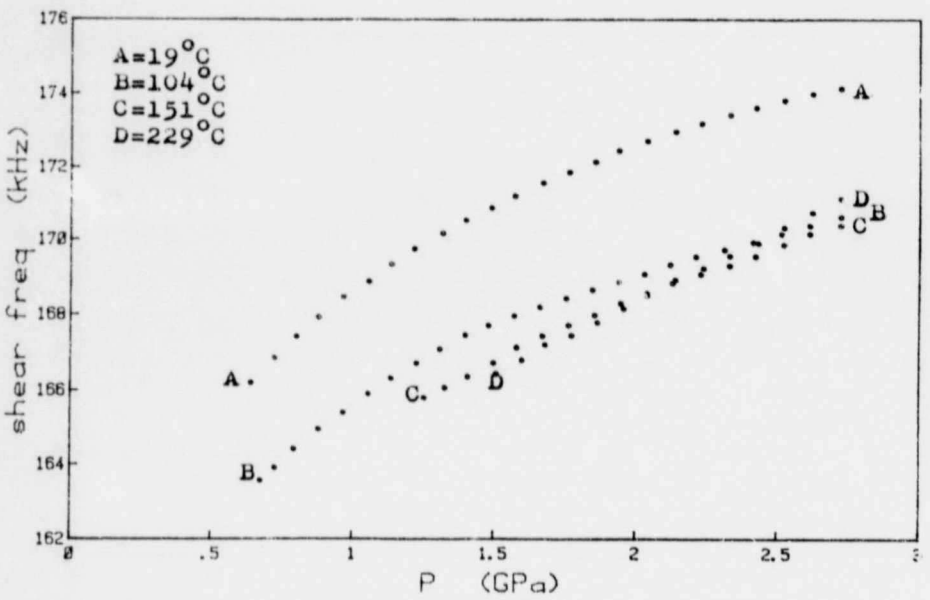

Fig. 5.2.3 9658 GC: Isotherms for the shear frequency vs pressure

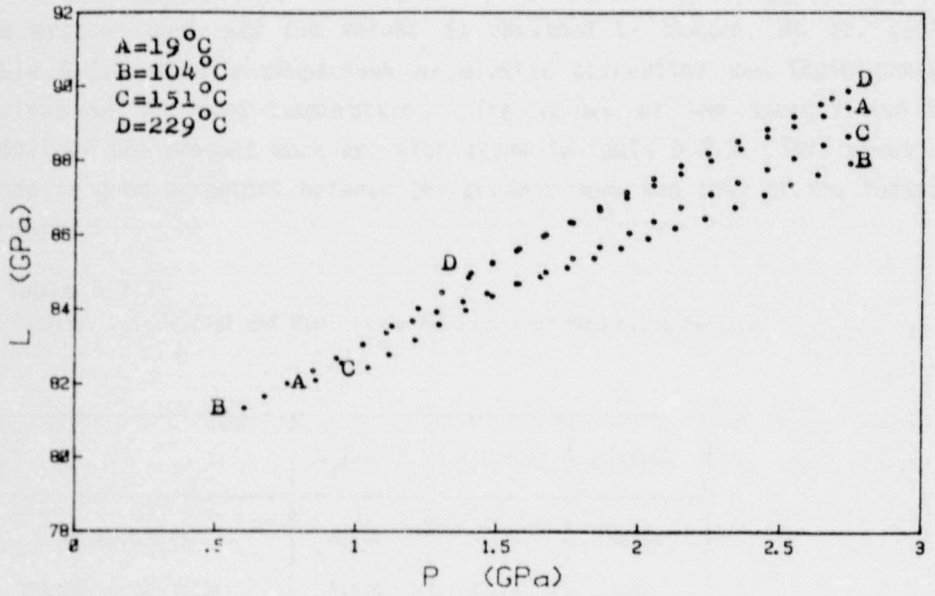

Fig. 5.2.4 9658 GC: Longitudinal modulus vs pressure

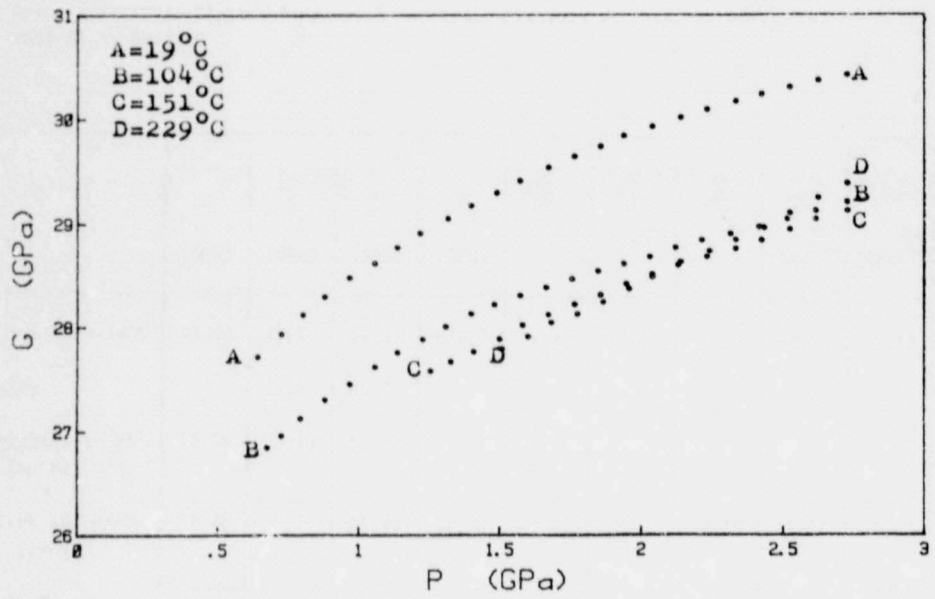

Fig. 5.2.5 9658 GC: Shear modulus vs pressure

Table 5.2.1 compares the density and phase velocities of this material in the present work and the values as obtained by Nakano, et al. (1978). Table 5.2.2 shows a comparison of elastic properties and their pressure derivatives at room temperature. The values of the Young's and bulk moduli of the present work are also shown in table 5.2.3. This shows that there is good agreement between the present work and that of the indicated workers.

Table 5.2.1
Density, Longitudinal and Shear Phase Velocities of 9658 Glass Ceramic

	V_ℓ(km/s)	V_t(km/s)	ρ(g/cc)
Present Work	5,446	3,178	2,553
Nakano et al (1987)	5,580	3,179	2,52

Table 5.2.2
Room Temperature Elastic Properties and their Pressure Derivatives of 9658 Glass Ceramic

	L (GPa)	G (GPa)	E (GPa)	B (GPa)	$\frac{dL}{dP}$ P=0	$\frac{dG}{dP}$ P=0	$\frac{dB}{dP}$ P=0	$\frac{d^2L}{dP^2}$ P=0 (GPa^{-1})	$\frac{d^2G}{dP^2}$ P=0 (GPa^{-1})	$\frac{d^2B}{dP^2}$ P=0 (GPa^{-1})
Present Work-19°C	77,00	26,22	65,12	42,27	6,69	2,70	3,17	-0,79	-0,43	-0,14
Corning		25,5	64,1							
Harrington et al (op cit)	77,96	25,39	63,91							
Gerlich and Hart (1984)	77,76	26,34	65,53	42,64	5,48	2,31	2,40	-1,92	-0,69	-1,00
Nakano et al (op cit)		25,46	16							

Figures 5.2.6 and 5.2.7 contain the variation of C_{11} and C_{44} with pressure, obtained by applying Fritz's method to the data of figures 5.2.4 and 5.2.5. Table 5.2.3 is a summary of the properties of this glass ceramic as being fitted with quadratic and cubic polynomials. It is important to note that the polynomials are only valid in the pressure ranges as indicated. It is evident that the behaviour of the pressure derivatives of the elastic moduli of this machinable glass ceramic is analogous to that of crystalline solids, i.e., positive first and negative second derivatives and opposite to the case of fused quartz and other tetrahedrally coordinated glasses (Gerlich and Hart, op. cit.).

Figures 5.2.8-11 show Young's modulus, the Lamé constant, Poisson's ratio and the bulk modulus versus pressure, respectively. The curves of the various isotherms do overlap at some places. However looking at the temperature dependence of E and G of this glass ceramic produced by Nakano, et al. (op. cit.) it is evident that the variation in these moduli is very small between 0 °C and 300 °C (see figure 5.2.12).

Figure 5.2.13 shows the volume variation as derived from the bulk modulus' variation with pressure. The result obtained by Gerlich and Hart (1984a) is shown together with the present graph for comparison at room temperature in figure 5.2.14. The agreement between these two graphs is very good.

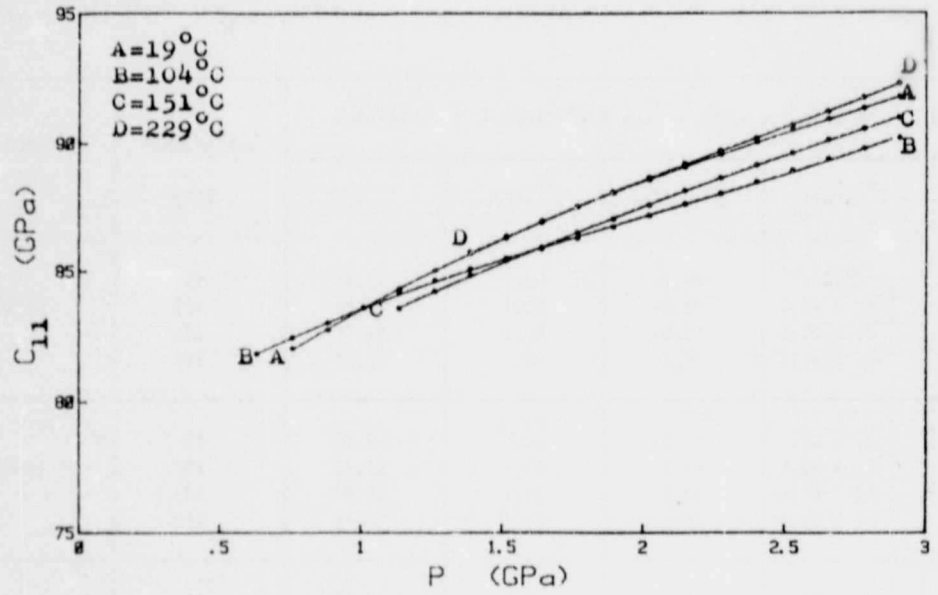

Fig. 5.2.6 9658 GC: C_{11} vs pressure

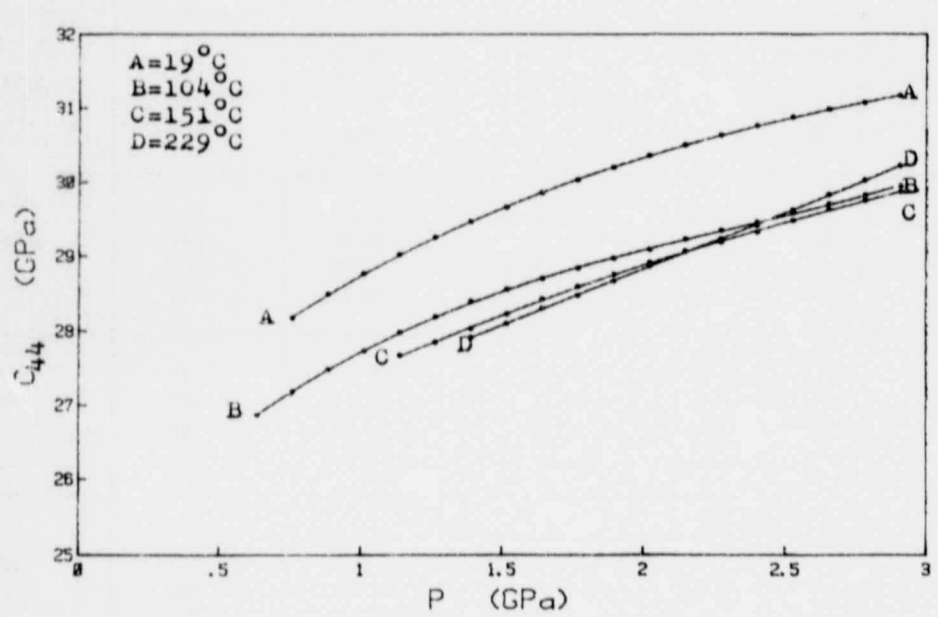

Fig. 5.2.7 9658 GC: C_{44} vs pressure